Science of the Total Environment 783 (2021) 146850

Contents lists available at ScienceDirect

Science of the Total Environment

journal homepage: www.elsevier.com/locate/scitotenv

Efficient recovery of phosphorus and sulfur from Anaerobic Membrane Bioreactor (AnMBR) permeate using chemical addition of iron and evaluation of its nutrient availability for plant uptake

Evan Heronemus [a,*], Kasuni H.H. Gamage [b], Ganga M. Hettiarachchi [b], Prathap Parameswaran [a]

[a] Department of Civil Engineering, Kansas State University, 2118 Fiedler Hall, 1701C Platt St., Manhattan, KS 66506, USA
[b] Department of Agronomy, Kansas State University, 2107 Throckmorton PSC, 1712 Claflin Road, Manhattan, KS 66506, USA

HIGHLIGHTS

- Efficient co-removal of phosphorus and sulfide in AnMBR by iron coagulation.
- Increased organic concentration has a negative impact on phosphorus removal.
- Coagulant aid is beneficial in removing phosphorus, as well as improved settling.
- Iron phosphate product acts as phosphorus sink, making it an ineffective fertilizer.

GRAPHICAL ABSTRACT

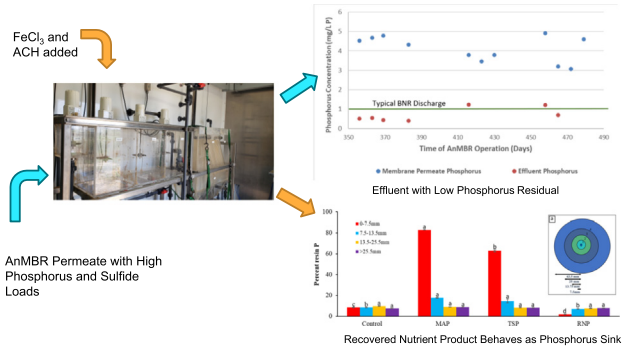

ARTICLE INFO

Article history:
Received 3 February 2021
Received in revised form 25 March 2021
Accepted 27 March 2021
Available online 1 April 2021

Editor: Huu Hao Ngo

Keywords:
Nutrient recovery
Anaerobic membrane bioreactor
Phosphorus removal
Chemical precipitation
Plant availability

ABSTRACT

Anaerobic membrane bioreactors (AnMBRs) represent an emerging environmental biotechnology platform with the potential to simultaneously recover water, energy, and nutrients from concentrated wastewaters. The removal and beneficial capture of nutrients from AnMBR permeate has yet to be fully explored, therefore this study sought to foster iron phosphate recovery through a tertiary coagulation process, as well as characterize the recovered nutrient product (RNP) and assess its net phosphorus release, diffusion, and availability for plant uptake. One of the primary goals of this study was to optimize the dose of the coagulant, ferric chloride, and coagulant aid, aluminum chlorohydrate (ACH), for continuous application to the coagulation-flocculation-sedimentation (CFS) unit of an AnMBR pilot plant treating municipal wastewater, through controlled bench-scale jar tests. Anaerobic systems present unique challenges for nutrient capture, including high, dissolved hydrogen sulfide concentrations, along with settleability issues. The addition of the coagulant aid increases settleability, while enhancing phosphorus removal by up to 20%, decreasing iron demand. Water quality analysis indicated that a variety of factors affect nutrient capture, including the COD (chemical oxygen demand) concentration of the permeate and the limiting coagulant dose. COD >200 mg/L was shown to decrease the phosphorus removal efficiency by up to 15%. A combination of inductively coupled plasma optical emission spectrometer (ICP-OES) elemental analysis, inductively coupled plasma mass spectrometer (ICP-MS) elemental analysis, scanning electron microscopy (SEM), X-ray diffraction (XRD), and X-ray absorption near-edge structure (XANES) spectroscopy analysis was used to characterize the P-rich RNP which revealed a 2.58% *w*/w phosphorus content and the lack of a well-defined crystalline structure. Detailed studies on resin extractable phosphorus to assess the plant uptake potential also demonstrated that iron-based P-rich RNPs may not be an effective fertilizer product, as they can act as a phosphorus sink in some agricultural systems instead of a source.

* Corresponding author.
E-mail address: eheronemus@ksu.edu (E. Heronemus).

https://doi.org/10.1016/j.scitotenv.2021.146850
0048-9697/

1. Introduction

Phosphorus and nitrogen are both essential nutrients for sustaining agriculture that can also become pollutants causing eutrophication downstream of point and non-point discharge such as municipal wastewater treatment plant effluent and runoff from agricultural and livestock operations. In freshwater ecosystems, phosphorus is more critical to causing pollution, as it is often the limiting nutrient (Schindler et al., 2008). Additionally, phosphorus is a resource that is depleting at a rapid rate as the world's population grows and farmers must produce more food to keep up with this demand. This creates a paradox of not having enough phosphorus to use as fertilizer, while high concentrations of phosphorus are polluting our water supplies (Sarvajayakesavalu et al., 2018). Thus, removal and capture of nitrogen and phosphorus from municipal and agricultural wastes, either separately or simultaneously as one commodity product, becomes a high priority. Various studies have shown progress in using agricultural wastes for food production applications (Sonmez et al., 2016; Turan et al., 2019; Klammsteiner et al., 2020). Biological nutrient removal (BNR) systems remove nitrogen and phosphorus together from municipal wastewater and produce a clean effluent that meets stringent total nitrogen and phosphorus discharge regulations, to produce effluent standards below 5 mg/L as N and 0.5 mg/L as P (Bashar et al., 2018). However, beneficial recovery of these valuable nutrients has limited success in BNR systems, as the nitrogen is transformed to nitrogen gas and phosphorus remains trapped in the settled BNR sludge, with biosolids land application being the dominant reuse option (Tchobanoglous et al., 2014).

There are several options available for a more effective recovery of phosphorus from wastewater, apart from removal. Precipitation of struvite ($MgNH_4PO_4$ or KNH_4PO_4) is a popular means to achieve simultaneous recovery of phosphorus and nitrogen as phosphate and ammonia in the form of a slow release fertilizer (Sengupta et al., 2015). The centrate from anaerobic digestion is an ideal environment for struvite to form, and chemicals such as magnesium chloride, hydroxide, or oxide are added to initiate and complete the production, while pH and temperature in the crystallizer are carefully controlled (Tchobanoglous et al., 2014; Pastor et al., 2010). The market for these slow-release fertilizers has allowed for several companies to develop various patented processes for struvite precipitation and crystallization, such as the Pearl, AirPrex, PHOSPHAQ, Phosnix, and Crystalactor processes, primarily working with municipal treatment plants to implement these processes and sell the products (Tchobanoglous et al., 2014; Giesen, 2009). However, struvite recovery efficiency is relatively low (10–50% P sequestration efficiency) and is typically possible only in municipal wastewater treatment plants with enhanced biological phosphorus removal (EBPR), where process parameters can be carefully maintained (Ewert et al., 2014; Egle et al., 2015). Additionally, research on recovery of struvite from other waste streams has been limited to pilot studies, and as stated previously, does not allow for separate capture of phosphorus and ammonia (Song et al., 2011; Rahman et al., 2014).

Chemical precipitation using lime, alum, and iron coagulants have also been shown to be an effective means of chemical phosphorus removal, however in a typical activated sludge treatment plant, these precipitates will be immobilized in the sludge as well (Sengupta et al., 2015). During direct anaerobic treatment of wastewater, nitrogen and phosphorus remain mobile as soluble ammonia and phosphate, which prevents their immobilization in the sludge and allows for exclusive capture of each of these nutrients in a subsequent downstream process, such as coagulation and flocculation.

Anaerobic membrane bioreactors (AnMBRs) represent an emerging environmental biotechnology platform with the potential to simultaneously recover water, energy, as well as nutrients from a variety of different concentrated wastewaters (Liao et al., 2006; Lin et al., 2013). AnMBRs combine the techniques of anaerobic biological treatment and membrane filtration, allowing for treatment of high strength wastewater to high effluent standards with a significantly reduced footprint (Lim et al., 2019). However, AnMBRs present another challenge for providing high quality effluent: the presence of sulfate-reducing bacteria (SRBs), which reduce the sulfate from the influent to hydrogen sulfide (Damodara Kannan et al., 2020).

Sulfur in the form of sulfide also poses water quality issues, consuming the dissolved oxygen and creating negative impacts on the water's taste and odor (Kristiana et al., 2010). This odor comes in the form of hydrogen sulfide gas, a harmful gas with an Occupational Safety and Health Administration (OSHA) exposure limit at 20 ppm (U.S. Department of Labor, 2020). There is no published standard for treated effluent wastewater sulfide concentration, but the EPA has a criterion of 0.002 mg/L according to their 1986 water quality "gold book" (U.S. EPA, 2007a). Sulfide and phosphate will both be present in municipal wastewater effluent after treatment through an anaerobic membrane bioreactor, requiring a tertiary treatment process for removal or recovery.

Coagulation of phosphate in the presence of sulfide is a novel process, of which only a few published studies exist (Yang and Bae, 2014; Dong et al., 2015). The study from South Korea demonstrated that sulfide and phosphorus removals were consistently above 99% and 80%, respectively, when using a ferric chloride ($FeCl_3$) dose at a molar ratio of 2.0 Fe^{3+}/S^{2-}, significantly greater than the stoichiometric ratio of 0.67 Fe^{3+}/S^{2-} required for sulfide removal (Yang and Bae, 2014). However, this study did not focus on recovery and characterization of these nutrients (Yang and Bae, 2014). Concomitant removal of sulfide and phosphorus from anaerobic centrates necessitates a higher coagulant dose, apart from other challenges such as the impact of residual organic matter in the permeate on nutrient capture efficiency and settleability of the precipitated product.

The addition of ferric chloride releases Fe^{3+} ions, which reduce to Fe^{2+} ions as they oxidize sulfide to sulfur (Yang and Bae, 2014; Gutierrez et al., 2010; Nielsen et al., 2005). These newly formed Fe^{2+} ions then precipitate out as iron sulfide (FeS) (Yang and Bae, 2014; Gutierrez et al., 2010; Nielsen et al., 2005). The released Fe^{3+} ions will also precipitate out phosphorus as $FePO_4{}^*2H_2O$ (Yang and Bae, 2014; Zhang et al., 2010). The mineral vivianite ($Fe_3(PO_4)_2{}^*8H_2O$) is also known to precipitate out from municipal wastewater in anaerobic systems when residual ferrous iron is present and is emerging as an alternative to struvite for phosphorus recovery (Wilfert et al., 2018; Rothe et al., 2016). Although Wilfert et al., 2018 was able to detect and quantify vivianite in municipal digested sludge, they did not assess its effectiveness in the soil as a phosphorus fertilizer product for plant uptake. Various iron hydroxide minerals, such as lepidocrocite and ferrihydrite, in addition to amorphous iron phosphate minerals are also known to precipitate out from wastewater dosed with iron (Wu et al., 2015).

Recovered nutrient products (RNPs) may differ in nutrient composition depending on the wastewater composition, wastewater characteristics and the treatment technologies applied. These recovered phosphorus rich nutrient products may contain high concentrations of other metals and anionic ligands, in addition to iron and phosphate, affecting phosphorus release and availability to plants. Although phosphorus in these iron-based P-rich RNPs could be a suitable phosphorus fertilizer source for some soils, their physical and chemical heterogeneous nature could lead to varying characteristics and behavior in soils. Characterization of these RNPs are important to understand the potential availability of nutrients when it is applied as a soil amendment or fertilizer. X-ray diffraction (XRD) (Ippolito et al., 2003; Massey et al., 2010; Zohar et al., 2018), scanning electron microscopy (SEM) examination coupled with energy dispersive X-ray spectroscopy (EDS) (Massey et al., 2010; Zohar et al., 2018; Battistoni et al., 2001), and X-ray absorption spectroscopy (Massey et al., 2018; Massey, 2019) have been used for product characterization in P recovery studies. Nutrient release, diffusion, and potential plant availability can be evaluated using soil incubation studies (Lombi et al., 2004; Hettiarachchi et al., 2008; Pierzynski and Hettiarachchi, 2018; Weeks and Hettiarachchi, 2020).

The pilot scale gas sparged AnMBR (1000 gal/day capacity) that was successfully operated by this research team at Fort Riley, Kansas for over 18 months also investigated the recovery of nutrient products, in the form of iron phosphates and iron sulfides from the permeate, using a coagulation-flocculation-sedimentation (CFS) unit (Lim et al., 2019). The objectives of this study were fourfold: to optimize the coagulant doses through batch jar tests of synthetic AnMBR permeate to achieve simultaneous removal of phosphorus and sulfide at varying chemical oxygen demand (COD) concentrations, to adjust the coagulant dosage for actual AnMBR permeate through additional batch jar tests, to evaluate whether the phosphorus and sulfide recovery goals can be achieved consistently during continuous operation of the pilot scale AnMBR's CFS unit, and to characterize the solid recovered nutrient products and evaluate its transformations in soil, through detailed soil studies for its phosphorus release rate and potential availability for plant uptake.

2. Materials and methods

2.1. Bench scale jar testing

When the AnMBR was not operational to provide permeate, Manhattan Wastewater Treatment Plant's secondary clarifier effluent was collected to be used as the model permeate. Sulfide, ammonium, and total phosphorus were added to the effluent to reach the desired levels that mimicked the AnMBR permeate from the pilot scale demonstration: 5 mg/L P, 40 mg/L NH_4-N, and 28.2 mg/L sulfide-S^{2-}. Next, the COD was adjusted to the appropriate concentration, with three levels tested: 22.8 mg/L, 45 mg/L, and 200 mg/L. The lowest COD concentration (22.8 mg/L) represents the average COD from the Manhattan wastewater clarifier effluent. To achieve the 45 mg/L and 200 mg/L concentrations of COD, volatile fatty acids (VFAs) were used to increase the COD of the synthetic permeate. Based on actual distribution of VFAs in the pilot scale AnMBR permeate from Ft. Riley, as quantified by high performance liquid chromatograph (HPLC) analysis (Shimadzu Scientific, USA), acetic acid and isovaleric acid were added to increase the COD level to 45 mg/L, and a combination of acetic acid, isobutyric acid, isovaleric acid, and valeric acid was added to increase the COD to 200 mg/L (Evans et al., 2018). The HPLC (Shimadzu LC-20AT, USA) uses an Aminex HPX-87H column (Bio-Rad Laboratories, USA) to separate the organic acids and alcohols which then were detected by a photo diode array and refractive index detectors (Lim et al., 2019). It should be noted that the sulfide addition was made after the COD was dosed to the appropriate levels based on VFA data, so the sulfide COD is not factored in. Once the synthetic permeate was appropriately dosed, initial conditions of dissolved iron, total phosphorus, sulfide, and pH were recorded. The pH of the synthetic permeates ranged from 7 to 8 based on the condition of the collected wastewater effluent.

Stock solutions of aluminum chlorohydrate (ACH) and $FeCl_3$ were prepared to reach densities of 0.267 g/mL and 1.411 g/mL respectively. The coagulants were then added from these stock solutions to four beakers filled with 1 L of the synthetic permeate. Each set of jar tests was divided into two sets, corresponding to four doses of the coagulant aid (ACH), ranging from 16.9 to 67.5 mg/L Al, for each of the two $FeCl_3$ doses, 121.5 and 182.2 mg/L Fe. This dosing matrix is shown explicitly in Table S1. The beakers were then rapidly mixed at 100 RPM for two minutes, after which the mixing speed was reduced to 30 RPM for 20 min. The jars were mixed using a Phipps & Bird Stirrer (model 7790–400). Once the slow mixing was completed, the contents of each jar were placed in 1000 mL graduated cylinders to settle for 30 min to evaluate sludge settleability. Once settleability was assessed, a sample was collected from the top 2 in. of the graduated cylinder and tested for turbidity. A liquid sample was collected from each cylinder and filtered through a 1.2 μm GF/C filter. The filtered samples were then tested for residual sulfide, total phosphorus, and dissolved iron. The unfiltered waste in each cylinder was finally tested for pH.

2.2. Bench scale analytical methods

Initial and residual dissolved sulfide tests were conducted using the USEPA Methylene Blue Method (Method 8131). Dissolved iron tests were conducted using USEPA FerroVer Method (Method 8008). A HACH DR 1900 spectrophotometer was used for dissolved sulfide and iron analyses. For the jar tests at 22.8 mg/L COD, total phosphorus was measured before and after coagulation using an inductively coupled plasma optical emission spectrometer or ICP-OES (720-ES, Varian, Santa Clara, CA). However, for the remaining tests, HACH TNT 843 kits (concentration range 0.05–1.5 mg/L as P) were used to measure total phosphorus. Previous testing in this lab has shown these two methods to give results within 15% of each other (Table S2). COD concentrations were verified using HACH TNT 820, 821, and 822 kits (concentration range 1–60 mg/L, 3–150 mg/L, and 20–1500 mg/L, respectively). The HACH kits were analyzed using the HACH DR 3900 spectrophotometer. Turbidity analysis was conducted using a HACH 2100Q portable turbidimeter. pH analysis was conducted using a VWR sympHony B10P pH benchtop meter.

2.3. Ft. Riley testing and pilot plant operation

Jar testing was conducted in the pilot scale AnMBR site using the same method as described in the Section 2.1, with the exceptions that actual permeate from the AnMBR was used rather than using a synthetic recipe and a cationic polymer was additionally added to aid settleability at a concentration of 1 mg/L. The polymer addition was to ensure adequate settleability for a wastewater derived product. Liquid grab samples were used to measure the phosphorus and sulfide levels at different stages of the treatment process (Lim et al., 2019). Residual sulfide was measured using similar methods employed for the bench scale jar test analysis, while total phosphorus was measured using an OI Analytical Alpkem RFA300 rapid flow analyzer (Lim et al., 2019). Ferric chloride and ACH concentrations of 110 mg/L as Fe, 30 mg/L as Al, and a cationic polymer at 1 mg/L were used for the continuous pilot scale CFS unit (Lim et al., 2019).

2.4. Characterization and plant uptake potential of recovered nutrient product

2.4.1. Product characterization

The original RNP sample, collected from the pilot scale AnMBR CFS unit during steady state operation, was freeze-dried and digested using USEPA method SW846-3051A (U.S. EPA, 2007c). The digestate was analyzed for the nutrient composition as well as for selected potentially toxic trace elements using an ICP-OES and an inductively coupled plasma mass spectrometer or ICP-MS (7500cx, Agilent, Santa Clara, CA). A powder XRD analysis was conducted to identify existing nutrient phases in the RNP using PANalytical Empyrean Multi-Purpose X-Ray Diffractometer (Spectris Company, Egham, Surrey, UK) with a copper anode material and generator settings of 35 eV and 20 mA. Due to expected amorphous nature of the products, scanning electron microscope (SEM) and energy dispersive spectroscopy analysis was also performed using a Hitachi S-3500 N scanning electron microscope equipped with a Model S-6542 absorbed electron detector (Hitachi Science Systems, Ibaraki, Japan) at an accelerating potential of 5 kV. X-ray absorption near-edge structure (XANES) spectroscopy analysis was conducted to further characterize the product at Sector 9-BM-B, Advanced Photon Source, Argonne National Laboratory, Argonne, IL. The RNP sample was diluted ten times using boron nitride. The sample was pelleted with a KBr Quick Press Kit (International Crystal Laboratories, Garfield, NJ) and carefully placed on a double-sided carbon tape (SPI Supplies, West Chester, PA) and placed on the sample holder. Six XANES scans were collected for the sample in fluorescence mode. Edge energy was calibrated using phosphorus pentoxide (P_2O_5). Background correction followed by the linear combination fitting of the reported spectra were done using previously collected standards

in Athena (Ravel and Newville, 2005) according to the concepts of Werner and Prietzel (2015).

2.4.2. Potentially plant available phosphorus determination

A 5-week long laboratory incubation study was conducted using an alkaline, mildly calcareous silt loam soil from Garden City, Kansas. Iron phosphate has limited solubility therefore, we chose this soil for our experiments. Soil was collected at the depth of 10 cm, air-dried and sieved to <2 mm. The pH of the soil was measured in a 1:10 soil: water extract (Watson and Brown, 1998) and available phosphorus (P) was measured by extraction with sodium bicarbonate (Olsen, 1954). The Cation Exchange Capacity (CEC) was determined by the displacement method (Soil Survey Staff, 2011); carbonates were determined according to Allison and Moodie (1965) and total P was determined according to Zarcinas et al. (1996), which is then modified to use a digestion block instead of a microwave. The Maximum Water Holding Capacity (MWHC) was measured using the protocol from Jenkinson and Powlson (1976). Total organic C was determined via the dry combustion method of Nelson and Sommers (1996). Soil texture was determined using a combination of a modification of the pipette method by Kilmer and Alexander (1949) and Method 3A-1 from the Soil Survey Laboratory's methods manual (Soil Survey Laboratory Staff, 2004).

Petri dishes (87 mm diameter and 11 mm height) were packed to a bulk density of 1.0 g cm^{-3} with 10% of the total deionized water needed for 55% soil's maximum water-holding capacity. Then by adding remaining deionized water slowly on to the packed soil, 55% maximum water-holding capacity was achieved. The plates were wrapped with Parafilm (Bemis Flexible Packaging, Neenah, WI), and left to equilibrate for 24 h at room temperature. The plates were unwrapped, and the powdered treatments were placed in the center of the plate, just below the soil surface and covering with soil. There were four treatments with four replicates as follows:

i. Unfertilized control soil sample;
ii. Mono ammonium phosphate (MAP, 11:23:0; 11% N–23% P–0% K_2O by weight): 7.5 mg P;
iii. Triple superphosphate (TSP, 0:20:0; 0% N–20% P–0% K_2O by weight): 7.5 mg P; and
iv. RNP (2.6% P by weight): 7.5 mg of P.

All fertilizer treatments received 7.5 mg P per petri plate. Petri dishes were closed and wrapped again with Parafilm (Bemis Flexible Packaging, Neenah, WI). Dishes were wrapped in aluminum foil and incubated (Precision Low Temp Incubator, Waltham, MA) in the dark at 25 °C. This 5 weeks' time indicates critical P uptake for cereal crops (Pierzynski and Hettiarachchi, 2018; Williams, 1948; Hettiarachchi et al., 2010).

Plates were opened at the end of 5 weeks and the soil was collected from 0 to 7.5, 7.5 to 13.5, 13.5 to 25, and 25 to 43.5 mm, from the point of application as concentric rings. Each sample was placed in a preweighed plastic specimen container (Fisher Scientific, Waltham, MA). The samples were oven dried quickly at 40 °C (Fisher Scientific drying oven, Waltham, MA). After drying, weight was recorded, and soils were ground gently with a mortar and pestle.

Total P for all samples was determined by aqua regia digestion (without H_2O_2 pretreatment) and analyzed via ICP-OES. Potentially plant available P was determined by the anion exchange resin (AER) technique (Myers et al., 2005) and quantified colorimetrically using a Beckman-Coulter DU-800 spectrophotometer (Brea, CA) (Murphy and Riley, 1962).

Percentage of resin P (PRP) for each dish section for all treatments were calculated according to the following equation (Pierzynski and Hettiarachchi, 2018):

$$PRP = \frac{PEP_i}{Total\ P_i} \times 100$$

where *i* is the dish section (1-4), REPi is the resin P concentration, and Total Pi is the total P concentration in the *i* dish section.

PROC MIXED procedure in SAS Institute (2011) were used to analyze the soil data. The experimental design was a complete randomized design. Least Significance difference method was used to compare all treatments at a 0.05 level of significance.

3. Results and discussion

3.1. Bench scale analysis with synthetic permeate

Bench scale testing was conducted to investigate changes in phosphorus and sulfide removal efficiencies as the coagulant doses and permeate COD concentrations were changed. The coagulant dosing matrix of $FeCl_3$ and ACH was developed by trial and error and evaluated based on a project goal to achieve 90% removal of total phosphorus from the municipal wastewater influent of the AnMBR (Evans et al., 2018).

3.1.1.1. Phosphorus removal - coagulant dosing effects. Previous studies have shown that adding iron salts for chemical phosphorus precipitation in traditional wastewater treatment plants and aerobic membrane bioreactors can achieve P removals greater than 90% (Caravelli et al., 2010; Wang et al., 2014). At a permeate COD of 22.8 mg/L, phosphorus removal was consistently greater than 96% for each ferric chloride dose, as shown in Fig. 1a. An increase in coagulant dose generally increased the phosphorus removal from less than 90% to 99%. Increasing the ferric chloride dose from 121.5 mg/L to 182.2 mg/L as Fe was shown to significantly increase the phosphorus removal for the synthetic permeate for COD values of 45 mg/L ($p = 0.005$) and 200 mg/L ($p = 0.006$). At this higher coagulant dose, the phosphorus removal percentage was always greater than 90%. The relationship between ferric chloride dose and phosphorus removal can be seen in Figs. 1a-c.

The impact of the coagulant aid, ACH, on settleability will be discussed in Section 3.3, but ACH is also known to be capable of achieving some phosphorus removal as a primary coagulant (Hatton and Simpson, 1985). As illustrated in Fig. 1, increasing the dose of ACH from 16.9 mg/L as Al to 33.7, 50.6, and 66.5 mg/L generally increased the phosphorus removal at each respective level, with an increase of over 20% seen at the highest COD level. This effect was more pronounced at the lower ferric chloride doses, where phosphorus removal efficiency was lower.

3.1.1.2. Phosphorus removal - COD effects. The bench scale study also shows a general decrease in phosphorus removal efficiencies as synthetic permeate COD increases, as can be seen by comparing Fig. 1a, b, and c. A significant decrease in phosphorus removal is seen when increasing the COD from 45 mg/L to 200 mg/L at the 121.5 mg/L ferric chloride dose ($p = 0.046$) and the 182.2 mg/L as Fe ferric chloride dose ($p = 0.001$). It is likely that this was caused by complexing of the organics with phosphate in aqueous form. There are conflicting studies on the impact of organics on settleability and phosphorus removal in coagulation (Omoike and Vanloon, 1999; Inskeep and Silvertooth, 1988; Zhou et al., 2008). Findings by Omoike and Vanloon (1999), as well as Inskeep and Silvertooth (1988) indicate that tannic acid can inhibit the precipitation of phosphorus. However, a study conducted by Zhou et al. (2008). has shown that tannic acid can behave as a coagulant aid in phosphorus removal to ferric chloride. A higher COD created a greater demand for the addition of coagulant to reach comparable P removal efficiencies to that of the lower COD samples. However, a phosphorus removal efficiency above the 90% threshold was still met when the highest concentrations of $FeCl_3$ and ACH were applied, with phosphorus concentrations consistently below 1.5 mg/L P.

3.1.2. Sulfide removal - coagulant dosing effects and impact of COD

Modeling in a previous study showed 98% removal of dissolved sulfide at a concentration of 7.6 mg/L from municipal wastewater with a

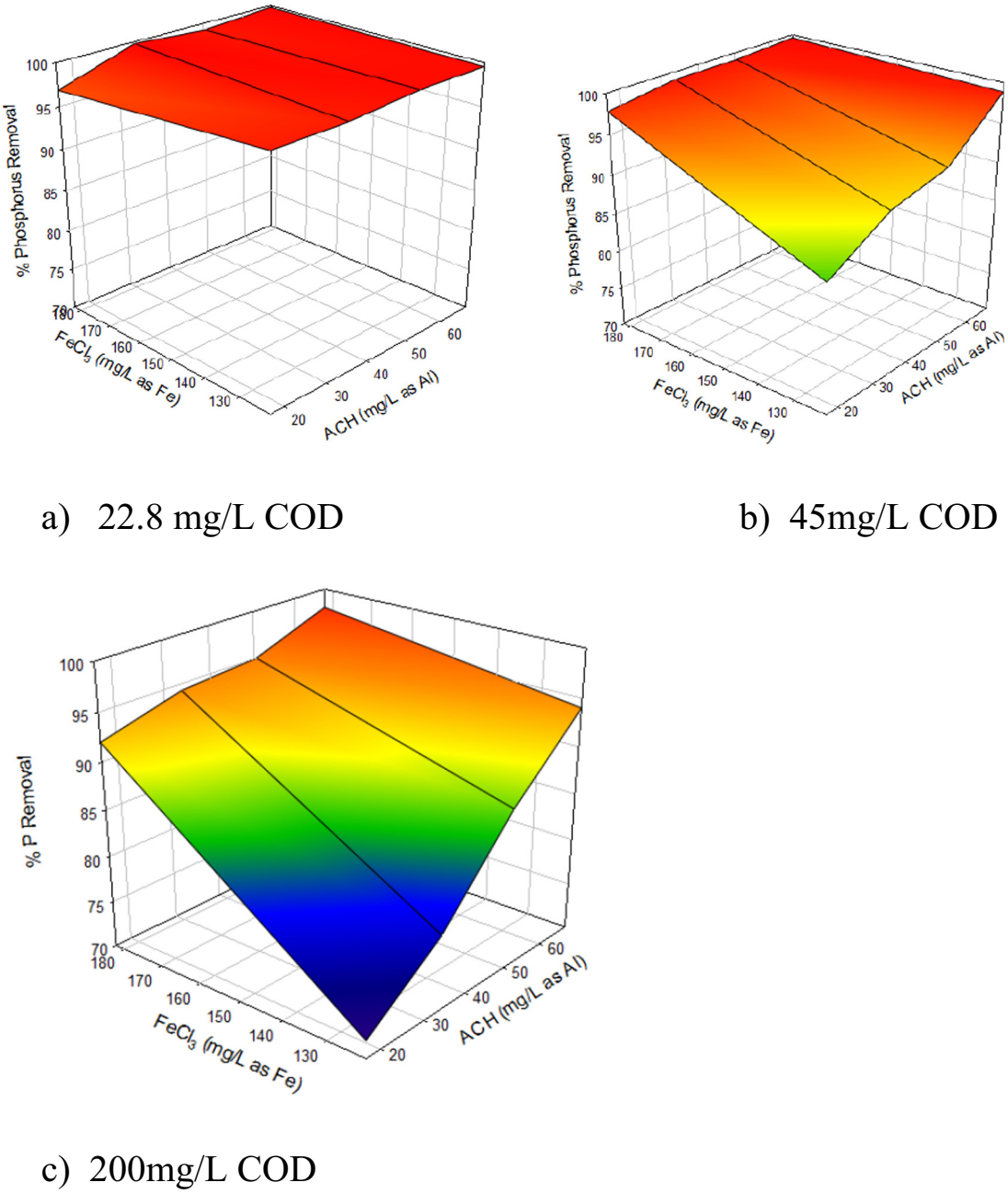

Fig. 1. Phosphorus removal efficiency as a function of coagulants $FeCl_3$ and ACH doses for jar tests at different COD levels. For increasing COD levels, Phosphorus removal efficiency dropped at the lower $FeCl_3$ (less than 150 mg/L as Fe) and ACH (less than 40 mg/L) doses.

dose of 30 mg/L $FeCl_3$ (Gutierrez et al., 2010). The jar testing setup, as described in Materials and Methods, consistently achieved a sulfide removal of 99.5% removal or greater for each ferric chloride and ACH combination. A 0.1 mg/L dissolved sulfide residual as S was chosen as a removal goal based on the capability of the AnMBR's CFS process (Lim et al., 2019). The two ferric chloride doses tested in this study, 121.5 mg/L Fe and 182.2 mg/L Fe, were well in excess of the previously mentioned stoichiometric ratio of 0.67 Fe^{3+}/S^{2-} at 2.5 and 3.7, respectively (Yang and Bae, 2014). Sulfide was consistently removed to concentrations below this goal at the higher ferric chloride dose, but the goal was not always met at the lower coagulant concentration. Although the residual reached after the coagulation process is significantly higher than the EPA criterion, it is likely to be further reduced downstream through sorption to clinoptilolite (a naturally occurring clay for ammonia adsorption from permeate) in the pilot scale AnMBR process train and some further losses by exposure to oxygen (Lim et al., 2019).

It should also be noted that increasing the ferric chloride dose did not always lead to increases in sulfide removal efficiency. This can be seen in Fig. 2 when examining the sulfide residual for the 45 mg/L COD waste at the two primary coagulant levels, the residual increases from approximately 0.02 mg/L to 0.05 mg/L ($p = 0.005$), with constant removal efficiency at >99.5%, as the iron dose increases. This could possibly indicate that there exists a threshold sulfide concentration, below which sulfide removal is easily achieved but competition for sulfide removal from other ions or organics might be maximized at a COD concentration of 45 mg/L.

There is not a clear trend between an increase or decrease in COD concentration and sulfide removal. However, as shown in Fig. 2, there appears to be an optimal removal of sulfide at a concentration

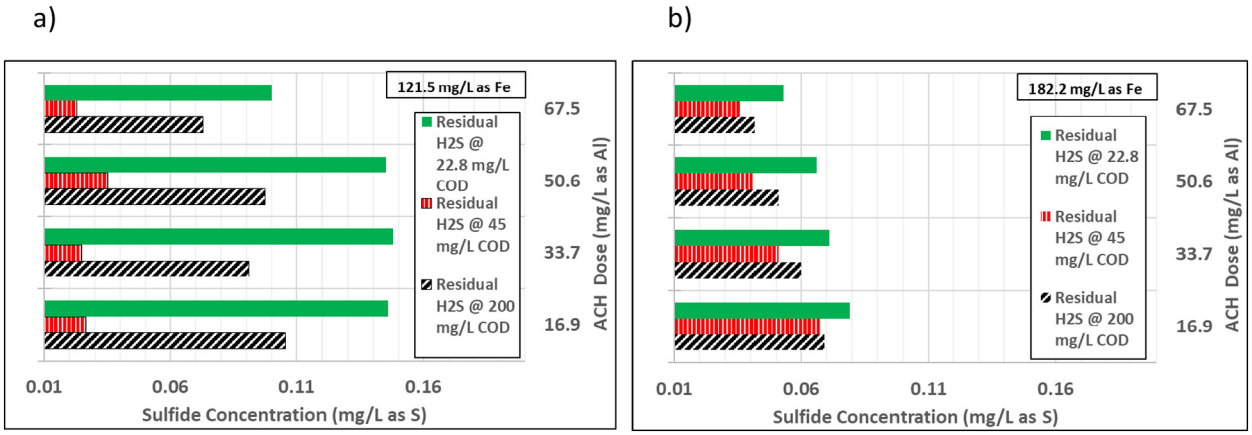

Fig. 2. Residual sulfide concentrations at various coagulant doses. The initial sulfide values in Fig. 2 (a) for 22.8, 45, and 200 mg/L COD at a ferric chloride concentration of 121.5 mg/L as Fe are 31.6, 26.6, and 28.0 mg/L as S, respectively. The initial sulfide values in Fig. 2 (b) for 22.8, 45, and 200 mg/L COD at a ferric chloride concentration of 182.2 mg/L as Fe are 28.3, 28.0, and 26.7 mg/L as S, respectively.

of 45 mg/L COD. At the lower ferric chloride dose of 121.5 mg/L as Fe, increasing the COD from 45 to 200 mg/L significantly increased the residual sulfide concentration ($p < 0.001$) from an average effluent residual of 0.027 mg/L to 0.126 mg/L, and decreasing the COD from 45 mg/L to 22.8 mg/L further significantly increased residual sulfide concentration ($p = 0.008$) from an average of 0.027 mg/L to 0.225 mg/L. While the p values show that this finding cannot be discarded, further replicability of the experiments is needed to analyze the reasons for this trend. Changing the COD concentration from 22.8 to 45 and 45 to 200 mg/L at the higher ferric chloride concentration did not cause statistically significant effects, however the same trend can still be observed in Fig. 2. This could be due to the excess iron increasing the efficiency of sulfide removal at any given concentration of organics.

3.1.3. Settleability and turbidity removal

The effectiveness of ACH as a coagulant aid was also shown in these jar tests. Turbidity was shown to decrease with increases in the ACH dose, as settleability increases (Fig. S1). Meanwhile, $FeCl_3$ dose increase had little impact on the turbidity, illustrating the need for a coagulant aid. The COD of the waste also influenced settleability, with higher turbidity values seen at higher COD levels. This was accompanied by an increase in phosphorus removal with increasing ACH dose, as shown in the surface plots in Fig. 1a, b, and c.

3.1.4. pH effects

A correlation between decreasing pH after the coagulation process and the residual dissolved iron can be observed in Fig. S2. This is a well-known relationship from iron chemistry (U.S. Department of the Interior, 1962). In drinking water systems, iron coagulation has an operating range at pH levels between 5 and 8.5 (Crittenden and Harza, 2012). Since the pH decreases with increasing iron dose, there will be an upper bound on the ferric chloride dose that will increase precipitation of the phosphate and sulfide present without moving the pH below the operating range. The optimal pH of the permeate for precipitation would be at the higher end of the operating range, as the minimum solubility of ferric species occurs at a pH of 8.0 (Crittenden and Harza, 2012).

3.2. Fort Riley AnMBR pilot plant

3.2.1. Jar testing with AnMBR permeate

The increased phosphorus removal efficiency at the 182.2 mg/L Fe dose compared to the lower Fe doses was further confirmed from jar

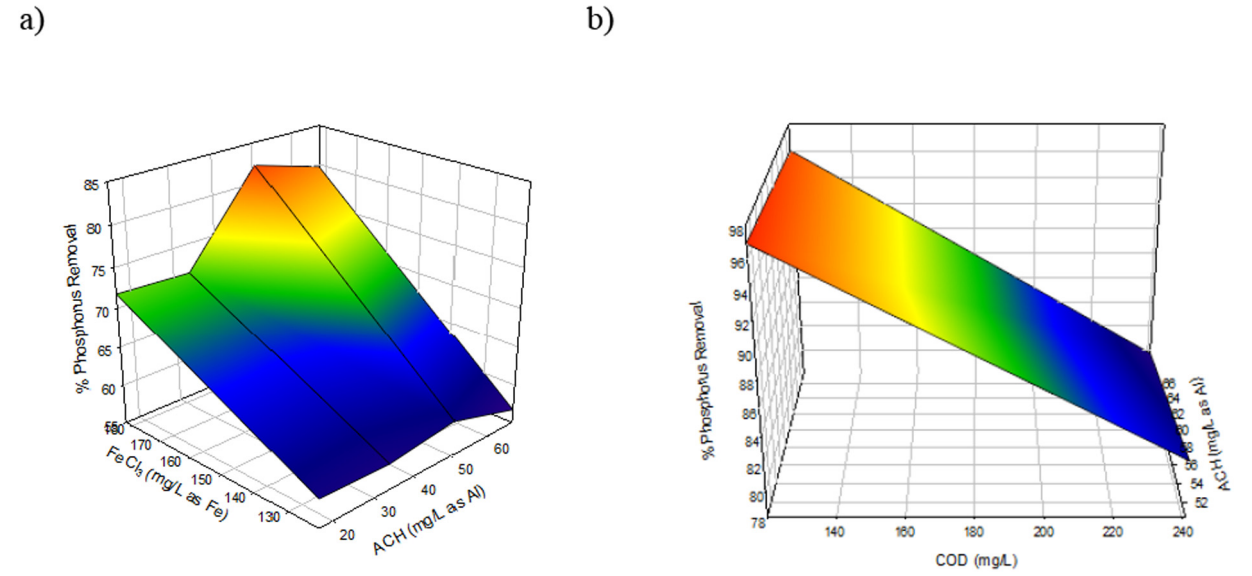

Fig. 3. Phosphorus removal efficiency from jar testing with actual AnMBR permeate. Panel a) shows increased phosphorus removal with increase in concentrations of the coagulants ferric chloride and ACH at 241 mg/L COD Panel b) shows the decrease of phosphorus removal with increasing COD concentration, at a fixed iron dose of 182.2 mg/L.

testing using the actual AnMBR permeate, as shown in Fig. 3 a). However, the phosphorus removal efficiency is still well short of the 90% goal at either iron concentration, when the COD of the permeate was at a high value of 241 mg/L. Jar testing was then performed to find if the phosphorus recovery would increase at lower COD levels, which indeed indicated P removals above 90% for the lower COD values, especially below 140 mg/L, as shown in Fig. 3 b. Increasing the COD from 120 mg/L to 241 mg/L decreased the phosphorus removal by over 15%. This decreased phosphorus removal efficiency is believed to be caused by organics complexing with phosphates, as previously discussed (Omoike and Vanloon, 1999; Inskeep and Silvertooth, 1988). Preliminary jar testing to evaluate coagulant dosing to achieve sulfide removal alone was not conducted, as sulfide removal using ferric chloride is already well established (Yang and Bae, 2014; Gutierrez et al., 2010; Nielsen et al., 2005).

3.2.2. AnMBR pilot plant continuous operation and effluent water quality

The coagulation-flocculation-sedimentation (CFS) unit integrated with the pilot scale gas sparged AnMBR began to operate successfully and continuously for a three-month period towards the end of long term operation (Evans et al., 2018). Data obtained from the pilot AnMBR plant supports the bench scale jar tests results: total phosphorus decreased from 4.2 ± 0.6 mg/L to 0.72 ± 0.36 mg/L and the sulfide concentration decreased from 27 ± 5 to 0.7 ± 1.7 mg/L through the CFS unit (Lim et al., 2019). It should be noted that this aforementioned phosphorus removal for the CFS system is only 83%, which is less than the project goal of 90%. However, this project goal was established for removing phosphorus throughout the entire pilot plant treatment train, and not solely the CFS unit. It was discovered early on in continuous operation that abiotic phosphorus removal occurs in the AnMBR prior to the CFS unit, with phosphorus concentrations decreasing from 7.0 ± 2.9 mg/L in the influent to 4.2 ± 0.6 mg/L in the permeate (Lim et al., 2019). Consequently, the coagulant doses were decreased from the bench scale jar test concentrations to 110 mg/L Fe and 30 mg/L Al for the lower quantum of phosphorus to be recovered in the CFS unit, further decreasing chemical costs. These decreasing phosphorus concentrations at the influent, membrane permeate, and effluent of the CFS system, throughout the operation of the AnMBR, can be seen in Fig. 4a. All total phosphorus effluent levels from the CFS unit during continuous operation met the 1.5 mg/L discharge limit, which has been

a)

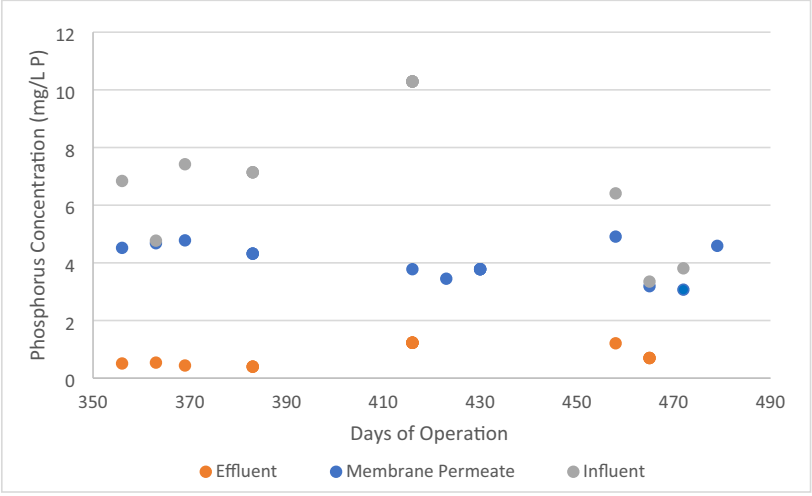

b)

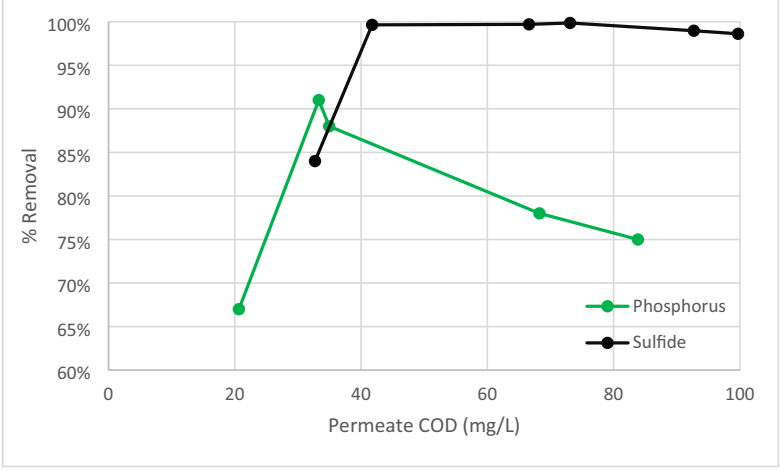

Fig. 4. a) Permeate and effluent phosphorus concentrations throughout the operation of the CFS system from day 356 of AnMBR operation to day 479. b) Phosphorus and sulfide removal by the CFS unit at various COD concentrations during continuous operation of pilot scale gas-sparged AnMBR.

proposed as a technology-based standard by the Kansas Surface Water Nutrient Reduction Plan (Kansas Department of Health and Environment, 2014). These effluent phosphorus concentrations are also similar to the discharge from a Biological Nutrient Removal (BNR) facility, which have a limit of technology (LOT) at 0.1 mg/L but typically discharge at a concentration close to 1 mg/L TP or below (U.S. EPA, 2007b). Sulfide was nearly always removed at or above 99% efficiency, but the 0.1 mg/L residual goal was not always met, with an average residual concentration of 0.7 mg/L, as mentioned previously (Lim et al., 2019).

The COD effects studied in bench scale jar tests with synthetic permeate were generally in agreement with data from continuous operation of the AnMBR. As shown in Fig. 4b, during continuous operation, the phosphorus removal efficiency generally dropped with increased COD concentration, while the sulfide removal efficiency showed little impact.

3.3. Recovered nutrient product characterization and plant uptake potential

The major and trace elemental composition of the freeze-dried product collected during continuous AnMBR pilot CFS operation is provided in Table S3. This product was rich in iron, aluminum, and sulfur, comprising approximately 19%, 20%, and 15%, respectively. Significant amounts of Al and Fe in these RNPs are predominantly from the iron and aluminum salts used for phosphorus precipitation in the CFS unit, which settled a product with 2.58% P. The selected trace elements concentrations in the freeze-dried product, as shown in Table S3, were low for this RNP. There are regulations and demands for fertilizer quality, efficiency, and composition, for each country (Breckenridge and Crockett, 1998). According to these regulations, the quality of fertilizers is understood as the maximum allowed concentration of contaminants and desired phosphorus content and its plant availability.

Based on the XRD analysis shown in Fig. 5, it appears that there are no identifiable diffraction lines for the RNP used for the incubation study. To have identifiable peaks in an XRD, there should be at least 2% (*w*/w) of relevant solid species in crystalline form. According to Stratful et al. (2001), increased retention time are associated with larger recovered crystals. This was especially true for complex wastewater matrices, where organic matter or other ions could interfere with crystallization by blocking crystal growth sites and delaying crystal formation (Massey et al., 2010). As shown in Fig. 5, the XRD obtained from a different batch of the same RNP has peak positions indicating that calcite ($CaCO_3$) is prominent and iron phosphates and aluminum oxides were present with lower peak intensities. The physical and chemical differences between products can be linked to the conditions of their formation (Massey et al., 2010).

Fig. 6 shows the data collected from the backscattered electron (BSE) images-Energy dispersive X-ray (EDX) analyzer. The atomic number sensitivity of BSE SEM images resulting in bright and less bright areas can be exploited to distinguish particles with different chemical composition and the EDX allows to get the elemental composition. The particles had an irregular, small, and homogeneous nature. According to the EDX of a selected particle of the RNP, the background is rich in Al (Fig. 6b) and the bright colored spots rich in S which could be elemental S (Fig. 6e). This coincides with the elemental composition obtained from the ICP-OES.

X-ray absorption near-edge structure spectroscopy analysis (XANES) of the RNP sample (Fig. 7) provides further evidence that this product is rich in iron adsorbed-P, such as goethite sorbed-P, and vivianite-like P. This result confirms the composition of this RNP. The lack of pre-edge suggests that these P solids do not have a well-defined crystalline structure, which supports the results of XRD analysis.

Selected physical and chemical properties of the soil used for the incubation study is given in Table S4, showing that the initial soil displayed characteristics of a mildly calcareous soil. Resin extractable P is a measure for potential plant available P concentration in soils (Myers et al., 2005). The greatest values of PRP were found within the 0- to 7.5 mm section followed by 7.5–13.5-,13.5- to 25- and 25- to 43.5-mm sections for MAP and TSP added treatments, as shown in Fig. 8. Recovered nutrient product amended treatment showed significantly lower PRP than control for the 0–7.5 mm section followed by similar PRP as control for all other sections. Fig. 8 shows that soil pH significantly decreased with P treatment relative to controls at the

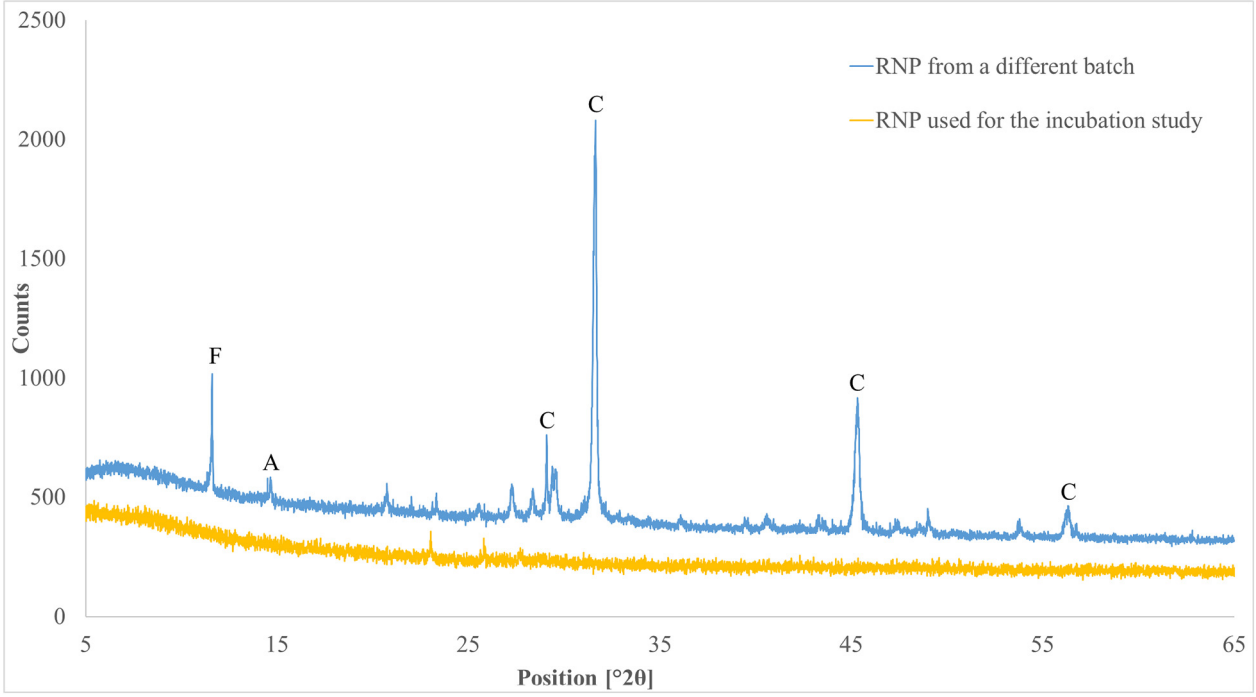

Fig. 5. XRD patterns for selected RNP samples. A, Al (hydr)oxide; C, calcite; F, Fe phosphate (samples collected from days 326 and 487 of pilot plant operation).

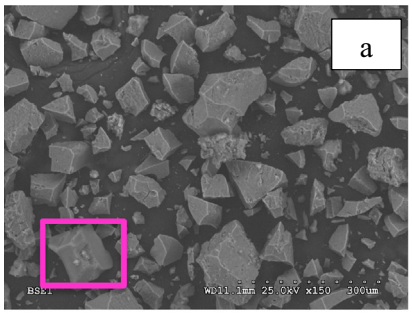

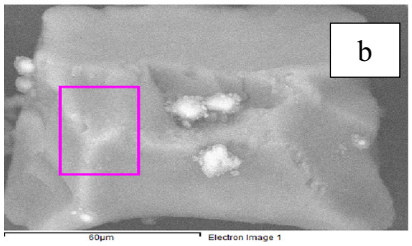

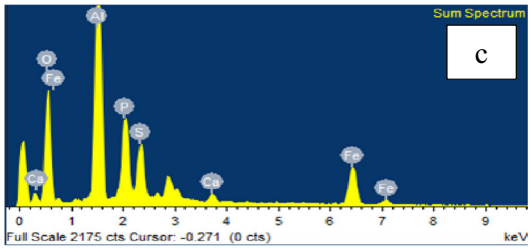

Element	Weight%	Atomic%
O	48.84	65.19
Al	25.70	20.34
P	9.13	6.30
S	6.31	4.20
Ca	0.97	0.52
Fe	9.04	3.46
Totals	100.00	

d

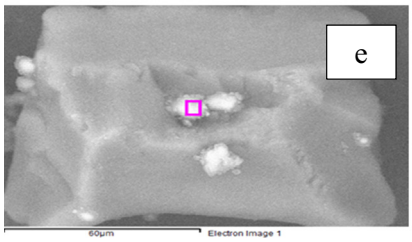

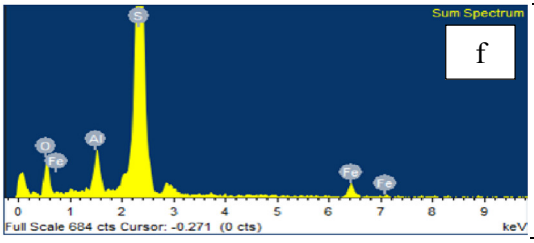

Element	Weight%	Atomic%
O	36.03	53.31
Al	4.06	3.56
S	56.42	41.65
Fe	3.49	1.48
Totals	100.00	

g

Fig. 6. (a) Backscattered electron (BSE) image of the RNP sample used for the incubation study. Area where selected to zoom in more is outlined in pink (b) More zoomed BSE image of the background of RNP sample. Area where the elemental analysis was conducted is outlined in pink (c) Elemental composition (d) Table of elemental composition (e) Zoom-in BSE image of the bright colored area of RNP sample. Area where the elemental analysis was conducted is outlined in pink (f) Elemental composition of the selected bright colored area (g) Table of elemental composition of the selected area.

0–7.5 mm section for MAP and TSP. Decrease in the pH of MAP compared to control is a result of acidification due to nitrification of ammonium-N contained within the phosphorus fertilizers (Hanson and Westfall, 1985). However, this reaction was limited by the overall buffering capacity of the soil carbonates (Lombi et al., 2004; Hettiarachchi et al., 2010). This likely causes more PRP in the 0–7.5 mm section in MAP than the other treatments. The phosphorus availability in calcareous soils is determined by phosphate adsorption and precipitation reactions with calcium carbonate. Dissolution of TSP causes direct soil acidification (Lindsay, 1979). Triple superphosphate, which contains monocalcium phosphate [$Ca(H_2PO_4)_2{\cdot}H_2O$], dissociates H^+ ion from the $H_2PO_4^-$ molecule and generates acidity. This leads to higher PRP in the 0–7.5 mm section in TSP than the RNP and control. Due to the indirect nature of soil acidification by MAP, it could persist for a longer time than TSP. The RNP was able to buffer the soil pH at its original pH. Presence of iron and aluminum oxides, which facilitate the sorption of phosphorus in soil, reduces the available phosphorus for plants. Aluminum or iron oxide-containing drinking water treatment residuals have been beneficially used as a Best Management Practice (BMP) to remove dissolved phosphorus from agricultural runoff water and therefore to enhance the surface water quality (Dayton et al., 2003). According to Novak and Watts (2004), application of water treatment residues (WTR) reduces the extractable soil P concentrations in a soil with excessive P concentrations and decreases the amount of P available for off -site transport. Applications of WTR with higher phosphorus sorption maximum values could be a part of a best management practice for biosolids or manure field applications (Ippolito et al., 2011). This product also shows a reduction of plant available P after application and therefore can be used as a P sink for this tested soil. In coastal sediments, previous studies have also shown that iron phosphates, including vivianite, act as phosphorus sinks

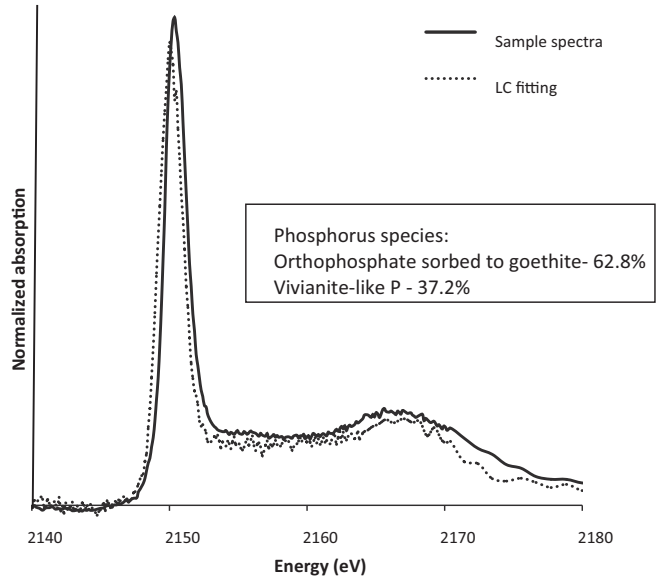

Fig. 7. Normalized Phosphorus K-edge XANES spectra with results of linear combination (LC) fitting for RNP used in incubation study.

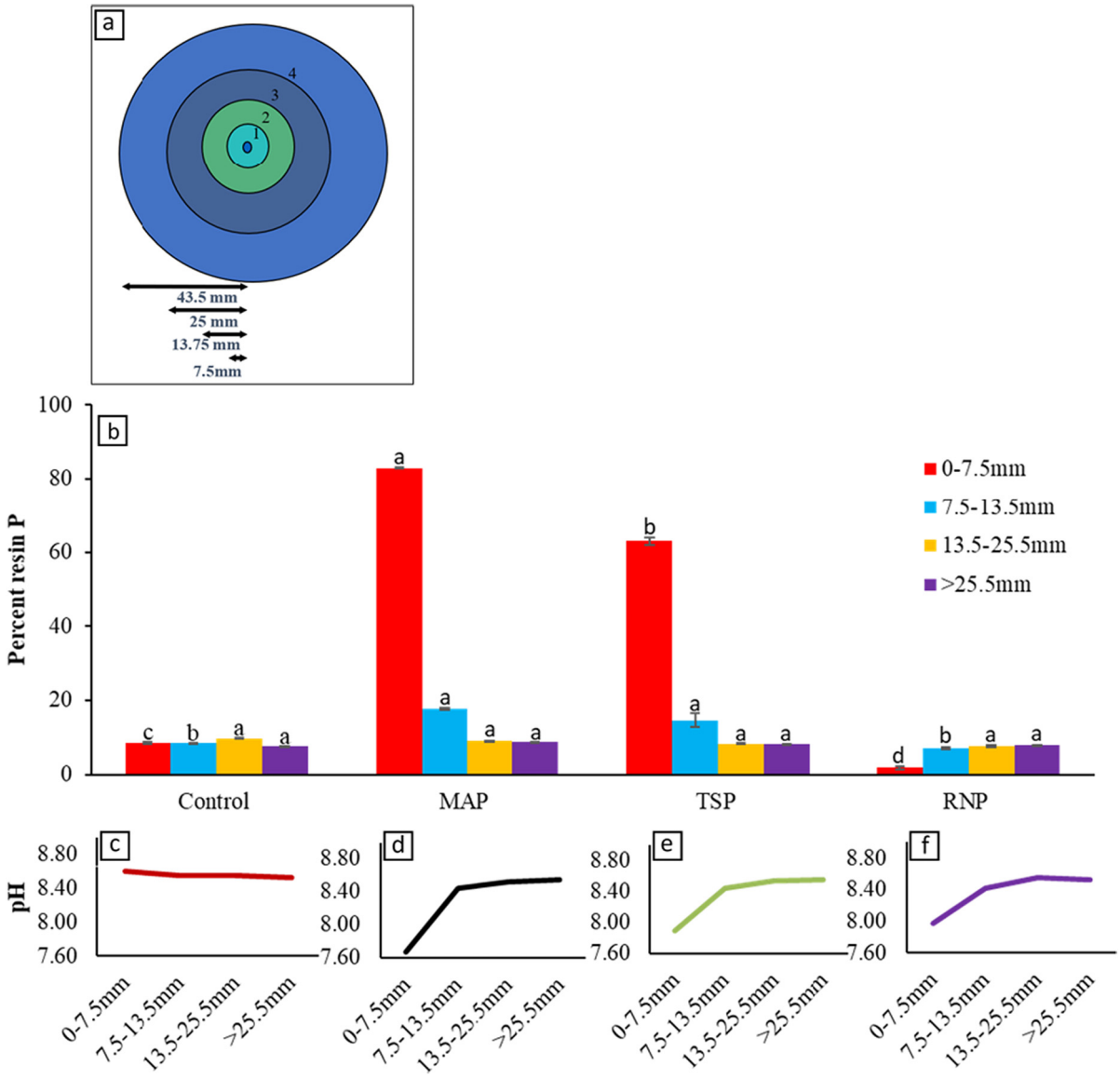

Fig. 8. (a) Illustration of soil sections in a petri dish in the incubation study (b) Percentage of resin P (PRP) for each dish section for all treatments. Standard error bars were averaged from the four replications for each dish section. Means within a soil section for each treatment containing the same letter are not significantly different at $p = 0.05$ according to Least significant difference method. MAP, monoammonium phosphate; TSP, triple superphosphate; RNP, recovered nutrient product (c) pH for each dish section for control (d) pH for each dish section for MAP (e) pH for each dish section for TSP (f) pH for each dish section for RNP.

(Dijkstra et al., 2014; Egger et al., 2015; Beauchemin et al., 2003; Weeks and Hettiarachchi, 2020). This indicates that vivianite recovery from wastewater may likely not lead to an effective fertilizer product despite growing interest motivated by the desire for an alternative to struvite recovery that has simpler process operation and does not require EBPR (Wilfert et al., 2018; Wu et al., 2019), as well as work showing it may be more efficiently separated from sludge than struvite (Wilfert et al., 2018). However, the reduced availability of P in the captured P-rich RNP could be beneficial in several other scenarios where excess phosphorus runoff could lead to huge ecosystem impacts such as eutrophication, harmful algal blooms and hypoxic zones in surface waters.

4. Conclusion

Bench scale jar testing with synthetic and actual AnMBR permeate has demonstrated that a variety of factors, including the coagulant and coagulant aid concentration, the pH of the permeate, and the permeate COD concentration, determines the optimum coagulant dosing in a system where phosphate and sulfide are both present. There is a threshold to the sulfide removal that can be economically achieved, and an increased iron dose can even decrease the sulfide removal efficiency at high enough Fe levels. To achieve the highest phosphorus removal, iron dosage is the limiting factor due to the preferential precipitation of sulfide over phosphate. An increased presence of organic COD can increase the iron dosage required even further. Due to settleability issues in anaerobic systems, the addition of aluminum chlorohydrate (ACH) as a coagulant aid was necessary. This study demonstrated that ACH increased settleability and decreased turbidity, in addition to aiding phosphorus removal and thus decreasing ferric iron demand. The bench scale results were successfully verified in a pilot scale coagulation-flocculation-sedimentation (CFS) system downstream of a gas sparged AnMBR with consistent removals of phosphorus and sulfide at or above 90% and 99%, respectively. The pilot system also confirmed that increasing permeate COD concentration decreased phosphorus removal efficiency but had little to no impact on the sulfide removal efficiency. Detailed and novel soil characterization studies on the RNPs from the

CFS unit demonstrated that P-rich RNPs may not be an effective slow release fertilizer product as widely perceived in recent literature, rather they likely act as a phosphorus sink in agricultural systems, which could be a beneficial application in itself in certain scenarios, especially pertaining to preventing eutrophication of water bodies from land applied phosphorus in phosphorus rich soils.

CRediT authorship contribution statement

Evan Heronemus: Methodology, Investigation, Writing – original draft. **Kasuni H.H. Gamage:** Methodology, Investigation, Writing – original draft. **Ganga M. Hettiarachchi:** Project administration, Writing – review & editing. **Prathap Parameswaran:** Project administration, Writing – review & editing.

Declaration of competing interest

The authors declare that they have no known competing financial interests or personal relationships that could have appeared to influence the work reported in this paper.

Acknowledgments

This research was supported by the United States Department of Agriculture (USDA)'s National Institute of Food and Agriculture (NIFA) under the Exploratory program Award # 2017-09353, as well as the Department of Defense Environmental Security Program [ESTCP Project number ER-201434], Kansas Agricultural Experiment Station [Contribution no. 21-091-J], and seed grant from Global Food System (GFS) program at Kansas State University. Graduate student research was supported by the Kansas National Science Foundation EPSCoR (Established Program to Support Competitive Research) First Award (#1000289) and the NSF National Research Traineeship (NRT) awards # 1828571. We also want to extend a thank you to Advanced Photon Source, Argonne National Lab, Chicago, IL. for providing the opportunity to use their synchrotron facilities. Special thanks to the beamline scientists Tianpin Wu, and George Sterbinsky at Sector 9 BM-B for their support during the data collection.

We thank Ms. Bernadette Drouhard (former undergraduate student, Department of Chemical Engineering, Kansas State University) and Ms. Megan Lehman (former undergraduate student, Department of Biological and Agricultural Engineering, Kansas State University) for helping with the bench scale jar tests of the real and synthetic permeate, as well as Mr. Kahao Lim (graduate student, Department of Civil Engineering, Kansas State University) for data collection from the pilot-scale CFS unit.

Appendix A. Supplementary data

Supplementary data to this article can be found online at https://doi.org/10.1016/j.scitotenv.2021.146850.

References

Allison, L.E., Moodie, C.D., 1965. Carbonate. In: Black, C.A., et al. (Eds.), Methods of Soil Analysis Part 2, 2nd ed. Agron. Monogr. 9. ASA, CSSA, and SSSA, Madison, WI, pp. 1379–1400.

Bashar, R., Gungor, K., Karthikeyan, K.G., Barak, P., 2018. Cost effectiveness of phosphorus removal processes in municipal wastewater treatment. Chemosphere 197, 280–290.

Battistoni, P., De Angelis, A., Pavan, P., Prisciandaro, M., Cecchi, F., 2001. Phosphorus removal from a real anaerobic supernatant by struvite crystallization. Water Res. 35, 2167–2178.

Beauchemin, S., Hesterberg, D., Chou, J., Beauchemin, M., Simard, R.R., Sayers, D.E., 2003. Speciation of phosphorus in phosphorus-enriched agricultural soils using X-ray absorption near-edge structure spectroscopy and chemical fractionation. J. Environ. Qual. 32, 1809–1819.

Breckenridge, R.P., Crockett, A.B., 1998. Determination of background concentrations of inorganics in soils and sediments at hazardous waste sites. Environ. Monit. Assess. 1998 (51), 621–656. https://doi.org/10.1023/A:1005808031053.

Caravelli, A.H., Contreras, E.M., Zaritzky, N.E., 2010. Phosphorous removal in batch systems using ferric chloride in the presence of activated sludges. J. Hazard. Mater. 177, 199–208.

Crittenden, J.C., Harza, M.W., 2012. MWH's Water Treatment: Principles and Design. 3rd edition. John Wiley & Sons, Hoboken, N.J.

Damodara Kannan, A., Evans, P., Parameswaran, P., 2020. Long-term microbial community dynamics in a pilot-scale gas sparged anaerobic membrane bioreactor treating municipal wastewater under seasonal variations. Bioresour. Technol. **310**, 123425.

Dayton, E.A., Basta, N.T., Jakober, C.A., Hattey, J.A., 2003. Using treatment residuals to reduce phosphorous in agricultural runoff. J. Am. Water Works Assoc. 95, 151–158.

Dijkstra, N., Kraal, P., Kuypers, M.M.M., Schnetger, B., Slomp, C.P., 2014. Are iron-phosphate minerals a sink for phosphorus in anoxic Black Sea sediments? PLoS One 9, e101139.

Dong, Q., Parker, W., Dagnew, M., 2015. Impact of FeCl3 dosing on AnMBR treatment of municipal wastewater. Water Res. 80, 281–293.

Egger, M., Jilbert, T., Behrends, T., Rivard, C., Slomp, C.P., 2015. Vivianite is a major sink for phosphorus in methanogenic coastal surface sediments. Geochim. Cosmochim. Acta 169, 217–235.

Egle, L., Rechberger, H., Zessner, M., 2015. Overview and description of technologies for recovering phosphorus from municipal wastewater. Resour. Conserv. Recycl. 105, 325–346.

Evans, P., Doody, A., Harclerode, M., Vila, P., Parameswaran, P., Lim, K., Bae, J., Shin, C., Lee, P.-H., Tan, A., McCarty, P., Parker, W., Guy, K., Page, M., Maga, S., 2018. Anaerobic Membrane Bioreactor (AnMBR) for sustainable wastewater treatment. Project ER-201434. Department of Defense Environmental Security Technology Program Final Report. Department of Defense.

Ewert, W., Hermanussen, O., Kabbe, C., Mele, C., Niewersch, H., Paillard, H., Stössel, E., Wagenbach, A., Steman, J., 2014. Sustainable Sewage Sludge Management Fostering Phosphorus Recovery and Energy Efficiency.

Giesen, A., 2009. P recovery with the Crystalactor process. Presentation in *BALTIC 21 Phosphorus Recycling and Good Agricultural Management Practice* (Berlin, Germany).

Gutierrez, O., Park, D., Sharma, K.R., Yuan, Z., 2010. Iron salts dosage for sulfide control in sewers induces chemical phosphorus removal during wastewater treatment. Water Res. 44, 3467–3475.

Hanson, R.L., Westfall, D.G., 1985. Orthophosphate solubility transformations and availability from dual applied nitrogen and phosphorus. Soil Sci. Soc. Am. J. 49, 1283–1289.

Hatton, W., Simpson, A.M., 1985. Use of alternative aluminium based chemicals in coagulation with particular reference to phosphorus removal. Environ. Technol. Lett. 6, 225–230.

Hettiarachchi, G.M., McLaughlin, M.J., Scheckel, K.G., Chittleborough, D.J., Newville, M., Sutton, S., Lombi, E., 2008. Evidence for different reaction pathways for liquid and granular micronutrients in a calcareous soil. Soil Sci. Soc. Am. J. 72, 98–110.

Hettiarachchi, G.M., Lombi, E., McLaughlin, M.J., Chittleborough, D.J., Johnston, C., 2010. Chemical behavior of fluid and granular Mn and Zn fertilisers in alkaline soils. Aust. J. Soil Res. 48, 238–247.

Inskeep, W.P., Silvertooth, J.C., 1988. Inhibition of hydroxyapatite precipitation in the presence of fulvic, humic, and tannic acids. Soil Sci. Soc. Am. J. 52, 941–946.

Ippolito, J.A., Barbarick, K.A., Heil, D.M., Chandler, J.P., Redente, E.F., 2003. Phosphorus retention mechanisms of a water treatment residual. J. Environ. Qual. 32, 1857–1864.

Ippolito, J.A., Barbarick, K.A., Elliott, H.A., 2011. Drinking water treatment residuals: a review of recent uses. J. Environ. Qual. 40, 1–12.

Jenkinson, D.S., Powlson, D.S., 1976. The effects of biocidal treatments on metabolism in soil—V: a method for measuring soil biomass. Soil Biol. Biochem. 8, 209–213.

Kansas Department of Health and Environment, 2014. Surface Water Nutrient Reduction Plan. pp. 1–18.

Kilmer, J., Alexander, L.T., 1949. Methods of making mechanical analyses of soils. Soil Sci. 68, 15–24.

Klammsteiner, T., Turan, V., Fernandez-Delgado Juarez, M., Oberegger, S., Insam, H., 2020. Suitability of Black Soldier Fly Frass as soil amendment and implication for organic waste hygienization. Agronomy (Basel) 10 (10), 1.

Kristiana, I., Heitz, A., Joll, C., Sathasivan, A., 2010. Analysis of polysulfides in drinking water distribution systems using headspace solid-phase microextraction and gas chromatography–mass spectrometry. J. Chromatogr. A 1217, 5995–6001.

Liao, B.-Q., Kraemer, J.T., Bagley, D.M., 2006. Anaerobic membrane bioreactors: applications and research directions. Crit. Rev. Environ. Sci. Technol. 36, 489–530.

Lim, K., Evans, P.J., Parameswaran, P., 2019. Long-term performance of a pilot-scale gas-sparged anaerobic membrane bioreactor under ambient temperatures for holistic wastewater treatment. Environ. Sci. Technol. 53, 7347–7354.

Lin, H., Peng, W., Zhang, M., Chen, J., Hong, H., Zhang, Y., 2013. A review on anaerobic membrane bioreactors: applications, membrane fouling and future perspectives. Desalination 314, 169–188.

Lindsay, W.L., 1979. Chemical Equilibrium in Soils. John Wiley & Sons, New York.

Lombi, E., McLaughlin, M.J., Johnston, C., Armstrong, R.D., Holloway, R.E., 2004. Mobility and Lability of phosphorus from granular and fluid Monoammonium phosphate differs in a calcareous soil. Soil Sci. Soc. Am. J. 68, 682–689.

Massey, M.S., 2019. X-ray spectroscopic quantification of Struvite and Dittmarite recovered from wastewater. J. Environ. Qual. 48, 193–198.

Massey, M.S., Ippolito, J.A., Davis, J.G., Sheffield, R.E., 2010. Macroscopic and microscopic variation in recovered magnesium phosphate materials: implications for phosphorus removal processes and product re-use. Bioresour. Technol. 101, 877–885.

Massey, M.S., Zohar, I., Ippolito, J.A., Litaor, M.I., 2018. Phosphorus sorption to aluminum-based water treatment residuals reacted with dairy wastewater: 2. X-ray Absorption Spectroscopy. J. Environ. Qual. 47, 546–553.

Murphy, J., Riley, J.P., 1962. A modified single solution method for the determination of phosphate in natural waters. Anal. Chim. Acta 27, 31–36.

Myers, R.G., Sharpley, A.N., Thien, S.J., Pierzynski, G.M., 2005. Ion-sink phosphorus extraction methods applied on 24 soils from the continental USA. Soil Sci. Soc. Am. J. 69, 511–521.
Nelson, D.W., Sommers, L.E., 1996. Total carbon, organic carbon, and organic matter. In: Sparks, D.L., Page, A., Helmke, P., Loeppert, R., Soltanpour, P., Tabatabai, M., et al. (Eds.), Methods of soil analysis Part 3 Chemical methods. ASA, CSSA, SSSA, Madison, WI.
Nielsen, A.H., Lens, P., Vollertsen, J., Hvitved-Jacobsen, T., 2005. Sulfide–iron interactions in domestic wastewater from a gravity sewer. Water Res. 39, 2747–2755.
Novak, J.M., Watts, D.W., 2004. Increasing the phosphorus sorption capacity of southeastern coastal plain soils using water treatment residuals. Soil Sci. 169, 206–214.
Olsen, Sterling R., 1954. Estimation of Available Phosphorus in Soils by Extraction With Sodium Bicarbonate. US Department of Agriculture, Washington, D.C.
Omoike, A.I., Vanloon, G.W., 1999. Removal of phosphorus and organic matter removal by alum during wastewater treatment. Water Res. 33, 3617–3627.
Pastor, L., Mangin, D., Ferrer, J., Seco, A., 2010. Struvite formation from the supernatants of an anaerobic digestion pilot plant. Bioresour. Technol. 101, 118–125.
Pierzynski, J., Hettiarachchi, G.M., 2018. Reactions of phosphorus fertilizers with and without a fertilizer enhancer in three acidic soils with high phosphorus-fixing capacity. Soil Sci. Soc. Am. J. 82, 1124–1139.
Rahman, M.M., Salleh, M.A.M., Rashid, U., Ahsan, A., Hossain, M.M., Ra, C.S., 2014. Production of slow release crystal fertilizer from wastewaters through struvite crystallization – a review. Arab. J. Chem. 7, 139–155.
Ravel, B., Newville, M., 2005. ATHENA, ARTEMIS, HEPHAESTUS: data analysis for X-ray absorption spectroscopy using IFEFFIT. J. Synchrotron Radiat. 12, 537–541.
Rothe, M., Kleeberg, A., Hupfer, M., 2016. The occurrence, identification and environmental relevance of vivianite in waterlogged soils and aquatic sediments. Earth Sci. Rev. 158, 51–64.
Sarvajayakesavalu, S., Lu, Y., Withers, P.J.A., Pavinato, P.S., Pan, G., Chareonsudjai, P., 2018. Phosphorus recovery: a need for an integrated approach. Ecosystem Health and Sustainability 4, 48–57.
SAS Institute, 2011. The SAS System for Windows Version 9.1.3. SAS Institute, Cary, NC.
Schindler, D.W., Hecky, R.E., Findlay, D.L., Stainton, M.P., Parker, B.R., Paterson, M.J., Beaty, K.G., Lyng, M., Kasian, S.E.M., 2008. Eutrophication of lakes cannot be controlled by reducing nitrogen input: results of a 37-year whole-ecosystem experiment. Proc. Natl. Acad. Sci. U. S. A. 105, 11254–11258.
Sengupta, S., Nawaz, T., Beaudry, J., 2015. Nitrogen and phosphorus recovery from wastewater. Current Pollution Reports 1, 155–166.
Soil Survey Laboratory Staff, 2004. Soil survey methods manual. Soil Survey Investigations Rep. No. 42 Version 4.0. National Soil Survey Center, Lincoln, NE.
Soil Survey Staff, 2011. Soil survey investigations report no. 45, version 2.0. In: Burt, R. (Ed.), Soil Survey Laboratory Information Manual. U.S. Department of Agriculture, Natural Resources Conservation Service.
Song, Y.-H., Qiu, G.-L., Yuan, P., Cui, X.-Y., Peng, J.-F., Zeng, P., Duan, L., Xiang, L.-C., Qian, F., 2011. Nutrients removal and recovery from anaerobically digested swine wastewater by struvite crystallization without chemical additions. J. Hazard. Mater. 190, 140–149.
Sonmez, O., Turan, V., Kaya, C., 2016. The effects of sulfur, cattle, and poultry manure addition on soil phosphorus. Turk. J. Agric. For. 40, 536–541.
Stratful, I., Scrimshaw, M.D., Lester, J.N., 2001. Conditions influencing the precipitation of magnesium ammonium phosphate. Water resEarch (Oxford) 35, 4191–4199.
Tchobanoglous, G., Stensel, H.D., Tsuchihashi, R., Burton, F.L., Abu-Orf, M., Bowden, G., Pfrang, W., 2014. Wastewater Engineering: Treatment and Resource Recovery. 5th edition. McGraw Hill, New York, N.Y.
Turan, V., Schröder, P., Bilen, S., Insam, H., Fernández-Delgado Juárez, M., 2019. Co-inoculation effect of Rhizobium and *Achillea millefolium* L. oil extracts on growth of common bean (*Phaseolus vulgaris* L.) and soil microbial-chemical properties. Sci. Rep. **9** (1) (15178-10).
U.S. Department of Labor, Accessed 22 February 2020. Hydrogen Sulfide. https://www.osha.gov/hydrogen-sulfide.
U.S. Department of the Interior, 1962. Chemistry of Iron in Natural Water. pp. 1–39.
U.S. EPA, 2007a. Quality Criteria for Water 1986 (Report No. 440/5-86-001). pp. 1–395.
U.S. EPA, 2007b. Biological Nutrient Removal Processes and Costs (Report No. 440/5-86-001). pp. 1–15.
U.S. EPA, 2007c. Method 3051A: microwave assisted acid digestion of sediments, sludges, soils and oils. Test Methods. USEPA.
Wang, Y., Tng, K.H., Wu, H., Leslie, G., Waite, T.D., 2014. Removal of phosphorus from wastewaters using ferrous salts – a pilot scale membrane bioreactor study. Water Res. 57, 140–150.
Watson, M.E., Brown, J.R., 1998. pH and lime requirement. In: Brown, J.R. (Ed.), Recommended Chemical Soil Test Procedures for the North Central Region. Missouri Agric. Exp. Stn. Univ. of Missouri, Columbia, MO, pp. 13–16.
Weeks, J.J., Hettiarachchi, G.M., 2020. Source and formulation matter: new insights into phosphorus fertilizer fate and transport in mildly calcareous soils. Soil Sci. Soc. Am. J. 84, 731–746.
Werner, F., Prietzel, J., 2015. Standard protocol and quality assessment of soil phosphorus speciation by P k-edge XANES spectroscopy. Environ. Sci. Technol. 49, 10521–10528.
Wilfert, P., Dugulan, A.I., Goubitz, K., Korving, L., Witkamp, G.J., Van Loosdrecht, M.C.M., 2018. Vivianite as the main phosphate mineral in digested sewage sludge and its role for phosphate recovery. Water Res. 144, 312–321.
Williams, R.F., 1948. The effects of phosphorus supply on the rates of intake of phosphorus and nitrogen and upon certain aspects of phosphorus metabolism in gramineous plants. Aust. J. Biol. Sci. 1, 333–341.
Wu, H., Ikeda-Ohno, A., Wang, Y., Waite, T.D., 2015. Iron and phosphorus speciation in Fe-conditioned membrane bioreactor activated sludge. Water Res. 76, 213–226.
Wu, Y., Luo, J., Zhang, Q., Aleem, M., Fang, F., Xue, Z., Cao, J., 2019. Potentials and challenges of phosphorus recovery as vivianite from wastewater: a review. Chemosphere (Oxford) 226, 246–258.
Yang, S., Bae, J., 2014. A feasibility of coagulation as post-treatment of the anaerobic fluidized bed (AFBR) treating domestic wastewater. Journal of the Korean Society of Water and Wastewater 28, 623–634.
Zarcinas, B.A., McLaughlin, M.J., Smart, M.K., 1996. The effect of acid digestion technique on the performance of nebulization systems used in inductively coupled plasma spectrometry. Communications in Soil Science and Plant Analysis: Soil Testing and Plant Analysis: Quality of Soil and Plant Analysis in View of Sustainable Agriculture and the Environment Part II. 27, pp. 1331–1354.
Zhang, T., Ding, L., Ren, H., Guo, Z., Tan, J., 2010. Thermodynamic modeling of ferric phosphate precipitation for phosphorus removal and recovery from wastewater. J. Hazard. Mater. 176, 444–450.
Zhou, Y., Xing, X.-H., Liu, Z., Cui, L., Yu, A., Feng, Q., Yang, H., 2008. Enhanced coagulation of ferric chloride aided by tannic acid for phosphorus removal from wastewater. Chemosphere 72, 290–298.
Zohar, I., Massey, M.S., Ippolito, J.A., Litaor, M.I., 2018. Phosphorus sorption characteristics in aluminum-based water treatment residuals reacted with dairy wastewater: 1. Isotherms, XRD, and SEM-EDS Analysis. J. Environ. Qual. 47, 538–545.